JULY 12–16
2020 VIRTUAL
JOINT AAPM | COMP MEETING
EASTERN TIME [GMT-4]

A Semi-Automatic Cardiac Substructure Segmentation Platform for Radiotherapy Planning CT

Erlei Zhang[1], Jinglei Li[3], Praveen Ranganath[2], Robert Timmerman[1], Prasanna Alluri[1], Mingli Chen[1], Weiguo Lu[1], Xuejun Gu[1]

[1]Department of Radiation Oncology, UT Southwestern Medical Center, Dallas, Texas
[2]Department of Radiology, UT Southwestern Medical Center, Dallas, Texas
[3]Guangdong General Hospital, Guangdong Academy of Medical Sciences, Guangzhou, China
Weiguo.Lu @UTSouthwestern.edu, Xuejun.Gu@UTSouthwestern.edu

MAIA Laboratory
UT Southwestern Medical Center
Radiation Oncology

INTRODUCTION

To evaluate radiotherapy cardiotoxicity, an accurate cardiac substructure segmentation on radiotherapy planning CT (pCT) is necessity. However, due to the poor contrast and low image resolution of radiotherapy planning CT (pCT), manually delineation of heart substructures is difficult. To overcome the bottleneck image quality of pCT, we developed an image-modality independent semi-automatic cardiac substructure segmentation platform.

METHODS

Figure 1 shows the outline of the proposed platform. This platform consists of two sections:

- Front-end user interface
  - Guide physicians to draw 11 anatomy regions of interest (ROIs) on pCT.
  - Obtain 11 landmarks via computing the average positions of ROIs
  - Submit 11 landmarks to the back-end pipeline
- Back-end cardiac segmentation
  - Atlas database
    - A contrast enhanced CT image (cCT),
    - Corresponding 11 landmarks
    - 7 substructures' contours
  - Cardiac segmentation module
    - pCT's and cCT's landmarks rigid alignment via a three-dimensional normal-distributions transform[1]
    - Computed a space transformation between the rigid-aligned landmarks from cCT and pCT via thin-plate splines (TPS) transformation algorithm[2]
    - Applied this TPS transformation to propagate 7 substructures' contours from cCT to pCT
- The segmented cardiac substructures on pCT can be used for radiotherapy cardiotoxicity evaluation.

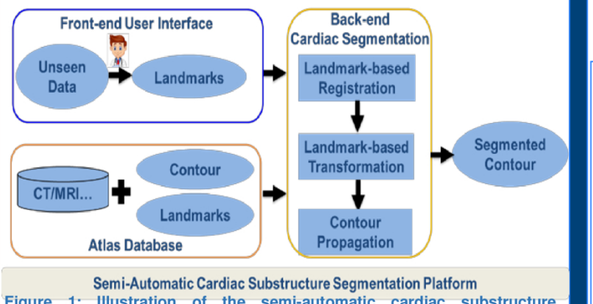

Figure 1: Illustration of the semi-automatic cardiac substructure segmentation platform for radiotherapy planning CT.

DATA AND LANDMARKS

- MM-WHS Dataset[3]
  - 6 patients
  - ~0.48 mm x 0.48 mm x 0.62 mm voxel size
- 7 Cardiac Substructures
  - left/right ventricular cavity (LV, RV)
  - left/right atrial cavity (LA, RA)
  - myocardium of the left ventricle (Myo)
  - ascending aorta (AA), pulmonary artery (PA)
- 11 Landmarks
  - apex, aortic/pulmonary valve
  - mitral/tricuspid valve
  - entrance of the superior/inferior vena cava
  - entrance of the right superior/inferior pulmonary vein
  - entrance of the left superior/inferior pulmonary vein

RESULTS

Fig.2 shows the altas (a) and segmentation result of a sample case (b). It can be seen that LA (green) and LV (blue) are accurate with minor changes compared to ground truth, Myo (red) and RV (magenta) are clinically acceptable RA (yellow), AA (cyan) and PA (orange) are less accurate. Table 1 presented the 7 substructures' Dice scores (mean ± standard deviation %) of our method, SAS and MAS on the MM-WHS dataset. The proposed method achieved the best performance (Dice ~90%) on the LA. Compared with SAS, our method achieved comparable results (Dice ~75%) on Myo and RA, and achieved better results on LA and RV. All the methods have relative poor performance on RA and PA. The reason may be that RA and PA have irregular shapes. We can observe that MAS achieved the best performance among those methods in all substructures as MAS combined multiple results from the set of atlases and has advantage in complex organs segmentation.

Overall, the proposed method achieves promising performance by taking advantage of the guidance of the landmarks. Especially, our method can propagate the contour from cCT to pCT as it is image modality independent, which has shown great potentials application for poor contrast and low resolution of radiotherapy pCT images.

Case	Myo	LA	LV	RA	RV	AA	PA
1	76.03	86.58	89.97	72.78	86.42	80.99	53.33
2	84.26	90.73	92.88	77.84	87.64	65.69	60.80
3	82.06	93.93	69.16	79.08	86.41	65.21	59.47
4	59.05	91.01	61.73	71.77	65.60	59.78	42.04
5	75.71	83.85	85.53	70.85	96.08	61.11	48.88
Ours	75.42±9.88	89.22±3.98	79.85±13.66	74.46±3.73	84.43±11.27	66.56±8.46	52.90±7.74
SAS	76.0±9.55	84.2±8.17	91.0±5.46	76.1±1.21	82.9±8.79	86.7±9.89	69.9±16.5
MAS	90.1± 2.42	92.0±4.13	96.7±1.25	87.2± 4.81	91.8±3.08	95.5±1.53	78.9±12.9

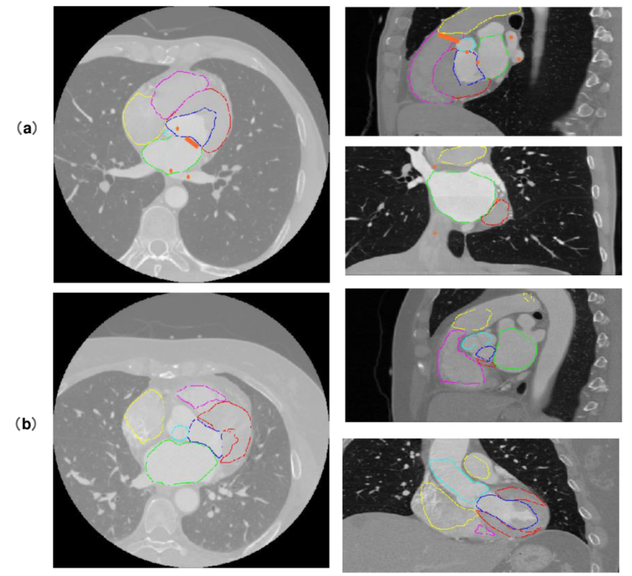

Figure 2: Three orthogonal views of the atlas and one segmentation case. (a) The parts of 7 contours and 11 landmarks (Orange) in the atlas. (b) Segmentation results of case 2, which has moderate Dice score among all cases.

CONCLUSIONS

The developed semi-automatic segmentation platform, which is image modality independent, yields accurate cardiac substructures delineation in evaluation cases. This accurate result indicate it the developed platform is promising for cardiotoxicity evaluation in radiotherapy.

REFERENCES

[1]Magnusson, Martin. "The three-dimensional normal-distributions transform: an efficient representation for registration, surface analysis, and loop detection." Diss. Örebro universitet, 2009.
[2]Whitbeck, Mark, and Hongyu Guo. "Multiple Landmark Warping Using Thin-plate Splines." IPCV 6 (2006): 256-263.
[3]Zhuang, Xiahai, et al. "Multiatlas whole heart segmentation of CT data using conditional entropy for atlas ranking and selection." Medical physics 42.7 (2015): 3822-3833.